Journal of Statistical Physics, Vol. 39, Nos. 5/6, 1985

Light Scattering Studies of the Ion Acoustic Instability in a Positive Column Plasma

R. E. Slusher,[1] C. M. Surko,[1] and C. A. Murray[1]

Light scattering is used to study the amplitude, spectrum, and angular distribution of the saturated state of the ion acoustic instability in a He positive column plasma. The ion acoustic waves are driven unstable by the electron current in the column. The properties of the saturated state are studied as a function of the concentration of hydrogen impurities which are found to be present in positive column plasmas. At concentrations of a few percent, the hydrogen ions can cause linear wave damping. Their role in saturating the instability by nonlinear processes is studied by varying the hydrogen concentration.

KEY WORDS: Light scattering; plasma instability; ion-acoustic waves.

1. INTRODUCTION

This study is focused on the relatively simple ion acoustic instability in an unmagnetized positive column plasma which is found to saturate by nonlinear processes at low levels of the wave amplitude. The ion acoustic waves are driven unstable in the positive column plasma by an electron current which feeds energy to the waves by inverse Landau damping. The threshold and saturated state of the instability are determined by a competition between wave damping and growth. The linear wave damping is primarily due to ion-neutral collisions in the partially ionized He positive column plasma. The growth rate first exceeds the damping rate in a region where the wave vectors K ($K = 2\pi/\lambda$ where λ is the wavelength) are of the order of the inverse electron Deybe wavelength λ_{De}. For example, for the experiments described here, the wave vector spectrum peaks at $K\lambda_{De} \sim 0.6$.

[1] AT&T Bell Laboratories, Murray Hill, New Jersey 07974.

0022-4715/85/0600-0755$04.50/0

At these wavelengths, probe measurements can be affected by the plasma screening around the probe (over distances of the order of λ_{De}), and it is difficult to be sure that the probe has not modified the spectrum or fluctuation level of the saturated state of unstable waves. The laser beam, used for the light scattering experiments described here, interacts with the plasma electrons by Thomson scattering, a very weak process which does not significantly perturb either the particles, the wave spectra, or the saturation level of the waves.

The ion acoustic instability has been studied by a number of different techniques including probes[1–4] and light scattering.[5,6] Even in similar plasmas, there is not complete agreement on the nature of the saturated state. For example, in positive column plasmas the angular distribution of wave vectors in the saturated state has been observed to extend about the current drive direction by no more than a few degrees in some experiments[2] and up to nearly 30° in others.[5] For plasmas not restricted to narrow cylindrical geometries and where ion-neutral collisions are not dominant, the saturation levels are significantly higher and the directional spread of the wave vectors in the saturated state extends to angles of $\pm 90°$ with respect to the current drive direction.[3] Applied magnetic fields further modify the angular distribution but these effects will not be considered here.

At present there is no complete understanding of the nonlinear processes which saturate the growth of the instability. Some of the processes to be considered include electron trapping in the wave potential, nonlinear ion Landau damping, ion-resonance broadening, and quasilinear effects on the electron velocity distribution. Renormalization theories,[7] which include all orders of the interdependence of wave amplitudes and particle velocity distributions, have made predictions which can be compared with experiments. However, at present, these theories do not include collisional damping. Numerical simulations[8,9] can also be compared with experiments. However, these are costly studies, and it is difficult to extend the parameter space and dimensionality of the simulation to make a good comparison with the experiment.

The light scattering study described here concentrated on nonperturbative measurements of the saturated state of the instability. In particular, the effects of small concentrations of light ion impurities (H ions in He plasmas) are shown to decrease the saturation levels without strongly modifying the angular extent or spectral distribution of waves in the saturated state.

The remainder of the paper is organized in the following way. A brief review of the theory for the ion acoustic instability in a positive column plasma is given in Section 2. The experimental apparatus and results for

the wave spectrum are described in Section 3. Since the first report of this study,[5] a more complete study of the effects of varying H ion concentration has been conducted and these new results are in Section 4. Initially the effects of light ions on the saturated state were interpreted as a nonlinear saturation effect due to ion-resonance broadening. In Section 5, an alternate explanation involving linear ion Landau damping by the light ions is presented, along with a discussion of the results and comparison with other experiments.

2. THE ION ACOUSTIC INSTABILITY IN A POSITIVE COLUMN PLASMA

The dominant terms in the complex dielectric constant $\varepsilon(\mathbf{K}, \omega)$ for the positive column plasma[1] are

$$\varepsilon(\mathbf{K}, \omega) = 1 - \frac{\omega_{pi}^2}{\omega(\omega + i\nu_{in})} + \frac{1}{(K\lambda_{\mathrm{De}})^2} + i\left(\frac{\pi}{2}\right)^{1/2}\left[\frac{1}{(K\lambda_{\mathrm{De}})^2}\left(\frac{\omega - \mathbf{K}\cdot\mathbf{v}_D}{Kv_{T_e}}\right)\right] \quad (1)$$

where ω is the frequency in radians, ν_{in} is the ion-neutral collision frequency, v_{T_e} is the electron thermal velocity, and $\mathbf{v}_D$ is the electron drift velocity (along the tube axis). The ion plasma frequency ω_{pi} is given by $(4\pi ne^2/M_i)^{1/2}$ where e is the electronic charge, M_i is the ion mass, and n is the plasma density. For all the experiments described here, the H^+ concentration is low enough that there are only small effects of this light ion mass on the resonant mode frequencies. From the zeros of this dielectric constant, the ion acoustic frequencies and wave vectors are found to be

$$\omega = \frac{c_s K}{[1 + (K\lambda_{\mathrm{De}})^2]^{1/2}} \qquad c_s = \left(\frac{kT_e}{M_i}\right)^{1/2} \quad (2)$$

and

$$K = K_{\mathrm{R}} + iK_{\mathrm{I}} \quad (2a)$$

where c_s is the ion acoustic phase velocity and K_{R} and K_{I} are the real and imaginary components of the wave vector K. At the onset of the instability, the most unstable frequency ω_M and wave vector K_M are calculated[1] to be

$$\omega_M = \frac{\omega_{pi}}{\sqrt{3}} \quad (3)$$

and

$$K_M = \frac{1}{\sqrt{2}\,\lambda_{\mathrm{De}}} \quad (4)$$

and the quantity

$$\left(\frac{v_D}{v_{T_e}}\right)\left(\frac{\omega_{pi}}{\nu_{in}}\right)\sim 1 \tag{5}$$

Experimentally the saturated spectrum is peaked at nearly these values of frequency and wave vector and all frequencies and wave vectors are related by the dispersion relation, Eq. (2).

Typical values of the particle and wave velocities for the positive column plasma are shown in Fig. 2. At the phase velocity of the ion acoustic wave, the slope of the electron velocity distribution is positive resulting in growth of the wave by inverse-Landau damping. This growth can be expressed as a component K_{IG} of the imaginary part of the wave vector

$$K_{\mathrm{IG}}=\left(\frac{\pi}{8}\right)^{1/2}\frac{K(v_D\cos\theta-\omega/K)}{v_e}\sim 4\ \mathrm{cm}^{-1} \tag{6}$$

where $K\simeq K_R$ and θ is the angle between $\mathbf{v}_D$ and $\mathbf{K}$. The ion velocity distribution slope for the bulk He ions and H impurity ions is negative and results in wave damping. Due to the small mass of the H impurities, the ions with velocity at the wave phase velocity can be dominated by the impurities. In this case the damping can be expressed[10] as a wave number K_{IDH}, where

$$K_{\mathrm{IDH}}=c_{\mathrm{H}}\left(\frac{\pi}{8}\right)^{1/2}K\left(\frac{T_e}{T_i}\right)^{3/2}\left(\frac{M_{\mathrm{H}}}{M_{\mathrm{He}}}\right)^{1/2}\exp\left(\frac{-M_{\mathrm{H}}T_e}{2M_{\mathrm{He}}T_i}\right)\sim 0.7\ \mathrm{cm}^{-1} \tag{7}$$

The numerical estimates in Eqs. (6) and (7) are calculated for the positive column plasma at the peak of the experimentally observed unstable spectrum, the T_e/T_i ratio is estimated to be 30, and the hydrogen concentration c_{H} is taken as 1%. In this regime the wave damping due to ion-neutral collisions is also important and contributes to K_{I} as

$$K_{\mathrm{IDN}}\simeq\left(\frac{\pi}{8}\right)^{1/2}\frac{\nu_{in}}{c_s}\sim 0.4\ \mathrm{cm}^{-1} \tag{8}$$

The growth of the wave energy W in the z direction can now be expressed in terms of the linear growth and damping mechanisms [Eqs. (6), (7), and (8)] and an (as yet unspecified) nonlinear mechanism which we assume to be of the form $K_{\mathrm{INL}}W^2$. Then

$$\frac{dW}{dz}=2(K_{\mathrm{IG}}-K_{\mathrm{IDN}}-K_{\mathrm{IDH}})\,W+K_{\mathrm{INL}}W^2 \tag{9}$$

At equilibrium in the saturated state, the total wave growth is zero and the equilibrium wave energy will be

$$W_s = 2\left(\frac{K_{\mathrm{IDN}} + K_{\mathrm{IDH}} - K_{\mathrm{IG}}}{K_{\mathrm{INL}}}\right) \tag{10}$$

The predictions of this simple model will be compared with the experimental results.

3. EXPERIMENTAL APPARATUS AND RESULTS FOR THE SATURATED WAVE SPECTRUM

A schematic diagram of the experimental apparatus is shown in Fig. 1. The ion acoustic waves, shown schematically as bunched dots, are excited in the positive column portion of a He discharge between a hot cathode and water-cooled anode. The distance from cathode to anode is 140 cm, and the inside diameter of the tube is 7.5 cm. Initial results[5,6] were

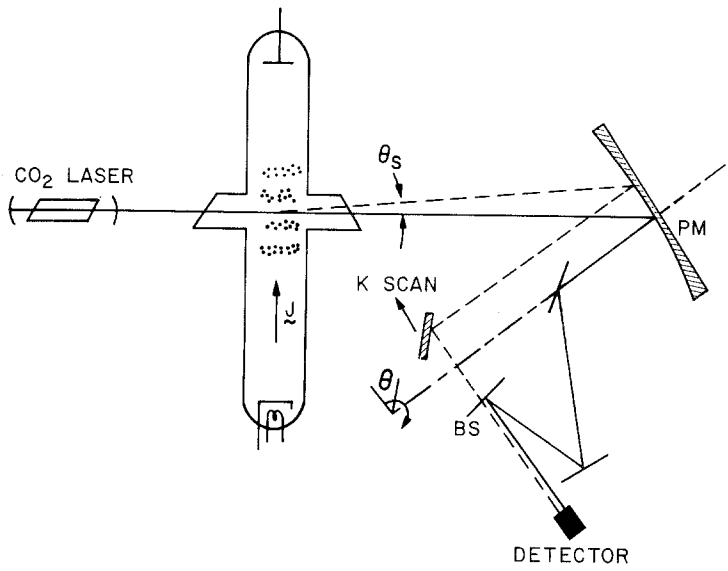

Fig. 1. A schematic diagram of the positive column plasma and CO_2 laser scattering arrangement. The electron current **J** flows from cathode to anode. The incident CO_2 laser beam shown as a solid line scatters at a small angle θ_s (shown as the dashed line). A parabolic mirror PM directs the scattered beams at various angles θ_s into a set of rays parallel to the axis of the parabolic mirror. The angular distribution in θ (in the plane containing **J** and perpendicular to the incident laser beam) is scanned by rotating the K-scan mirror about the axis of the parabolic mirror. A portion of the incident beam is combined with the scattered light for a particular K and θ at the beamsplitter BS and directed to the heterodyne detector.

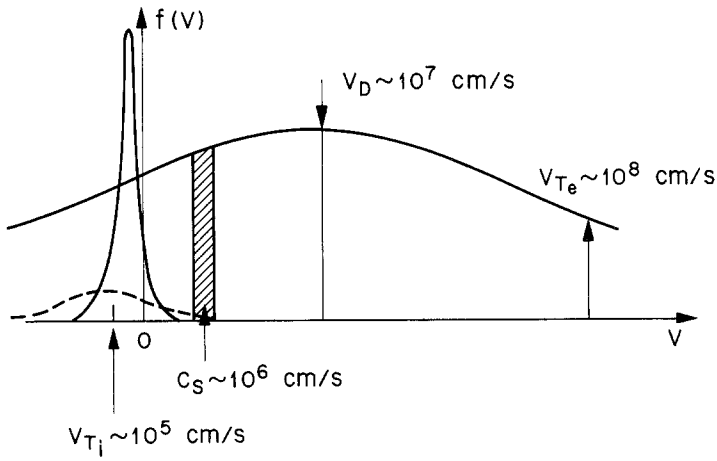

Fig. 2. The velocity distributions $f(v)$ for electrons and ions in a positive column plasma are shown along with orders of magnitude for the key parameters in characterizing the ion acoustic instability. The cross-hatched region is important for resonant interaction of electrons with the ion acoustic waves with phase velocity c_s. Hydrogen impurities have a broader velocity distribution (shown as the dashed line) than the bulk helium ions.

obtained with a water-cooled Pyrex tube and a flow rate of 0.7 torr-liter/sec. However, in order to minimize H impurity for the new results presented here, a quartz tube was used (which had lower OH concentration than Pyrex), liquid nitrogen cooling was used at times, and great care was taken to minimize H contamination from the vacuum system. The discharge current was in the range from 1 to 10 A, and the neutral gas pressure ranged from 0.01 to 0.15 torr. These conditions resulted in plasmas with densities n measured to be in the range from 10^{10} to 10^{11} cm^{-3}, electron temperatures T_e measured to be in the range from 4 to 6 eV, and ion temperatures estimated to be about 0.2 eV.

Accurate measurements of the saturated wave spectrum and the angular distribution of the wave vectors were made using the light scattering apparatus shown in Fig. 1. Light from a CO_2 laser operating at a wavelength of 10.6 μm, having a TEM_{00} mode with 20 W of CW power is focused into the plasma at a point 105 cm from the cathode. At this position the saturated state of the ion acoustic instability is fully developed. The laser was oriented in a direction perpendicular to the discharge current. Scattering from this light beam at angles of the order of 1° (corresponding to the Bragg angle for the ion acoustic wavelengths near 1 mm) was due to the electron density perturbation of the ion acoustic wave. The scattered light was heterodyne detected using a liquid-helium-cooled Ge:Cu photoconductor. The parabolic mirror shown in Fig. 1

collects the scattered light at various angles (corresponding to the spread of wave vectors in the saturated wave spectrum) and redirects the light parallel to a common axis. This allows a scan of the wavevector spectrum in a fixed direction of **K** by simple translation of a mirror. The angular distribution $W(\theta)$ of the waves in a plane containing the electron current and perpendicular to the incident laser is obtained by a rotation of a mirror pair about the center line of the parabolic mirror. The local oscillator for heterodyne detection is a small portion ($P_{LO} \sim 200$ mW) of the incident laser beam. The detected current through a load resistor forms a voltage which is amplified to obtain $V(K, \theta)$. This voltage is frequency analyzed using a spectrum analyzer. Typically the frequency spectrum corresponding to a particular set of K and θ values is peaked at a frequency between 10 and 20 MHz with a frequency width consistent with the K resolution of the scattering arrangement. The wave vector resolution is limited by the width a_0 of the laser beam in the plasma (a_0 is the radius to $1/e^2$ in power for the Gaussian profile of the laser beam) to $\Delta K_r/K$ equal to $2/a_0 K$. Typical values of $a_0 = 0.4$ cm yield $\Delta K_r \sim 5\ \text{cm}^{-1}$. For $K \sim 100\ \text{cm}^{-1}$, this corresponds to a frequency width of 0.5 MHz.

The measured angular and wave vector distributions[5] are shown in Fig. 3. These data include the finite wave vector resolution ($|\Delta K_r|/K \sim 5\%$ and $\Delta\theta/\theta \sim 10\%$). The detected voltage is proportional to a convolution of the actual spectrum of the line integral of $\tilde{n}(K, \theta)$ along the direction of the laser beam and the scattering resolution functions.[6] Because of the small scattering angle, there is no resolution across the plasma along the laser beam. Note that the spectra are broad in both K and θ. For a given K and θ, the frequency spectra are consistent with excitation of only the linear modes predicted by the dispersion relation in Eq. (2).

By varying the plasma current and gas pressure, the parameter v_D/v_{T_e} can be scanned in the region of the wave instability. The total wave energy normalized to the electron particle energy $\int [W(K, \theta)/nT_e]\, d\theta\, dK$ and the corresponding angular and wave vector distribution widths are shown in Fig. 4 as a function of v_D/v_{T_e}.[5] The wave energy saturates at low values, i.e., the wave energy is much less than the particle energy. The angular distribution $\Delta\theta$ (where $\Delta\theta$ is the angular width of $\tilde{n}(\theta)$ to $1/e$ points) also approaches a limiting value of about 30°.

4. HYDROGEN-ION IMPURITY EFFECTS

It was found that an important parameter determining the saturated wave energy was the concentration of H^+ impurity in the He^+ plasma. The data in Figs. 3 and 4 were taken without particular caution to eliminate H impurities which originate from water vapor in the system and

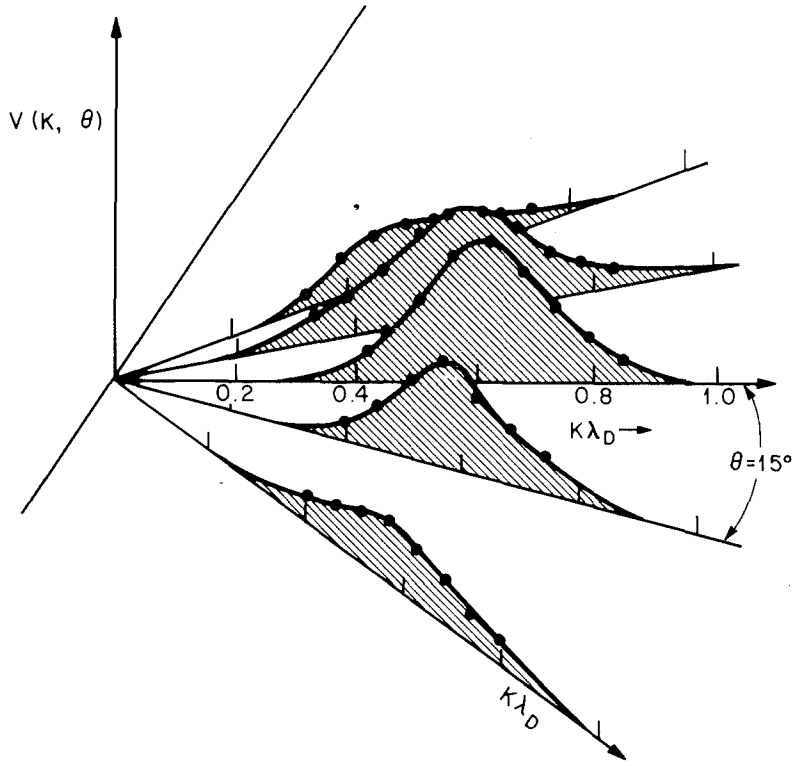

Fig. 3. The measured heterodyne voltage, $V(K, \theta)$, proportional to the electron density fluctuations of the unstable ion acoustic waves, is shown as a function of $K\lambda_{De}$ and θ. Scans in K at four values of θ ($\theta = 0, \pm 15°, \pm 30°$) are shown which include a resolution width of approximately 5% in $\Delta K_r/K$.

the OH content in the glass walls of the plasma tube. The effects due to H impurity were studied by minimizing the background levels of H and then introducing controlled quantities of H gas along with the He gas flow to the discharge. A number of techniques were used to minimize the H concentration. These included the use of quartz to replace Pyrex as a wall material, high-temperature baking and discharge cleaning of the quartz tube in order to minimize H_2O at the surface and remove OH from the wall near the surface in the quartz, liquid nitrogen cooling of the discharge tube walls, high flow rates of ultrapure He gas, Cu O-ring seals, and the introduction of a liquid nitrogen trap in the gas supply line. The amount of H impurity in the discharge was estimated from a measurement of the optical emission intensity of both neutral He at a wavelength of 6678 Å and neutral H at a wavelength of 6563 Å. Although the absolute level of H^+

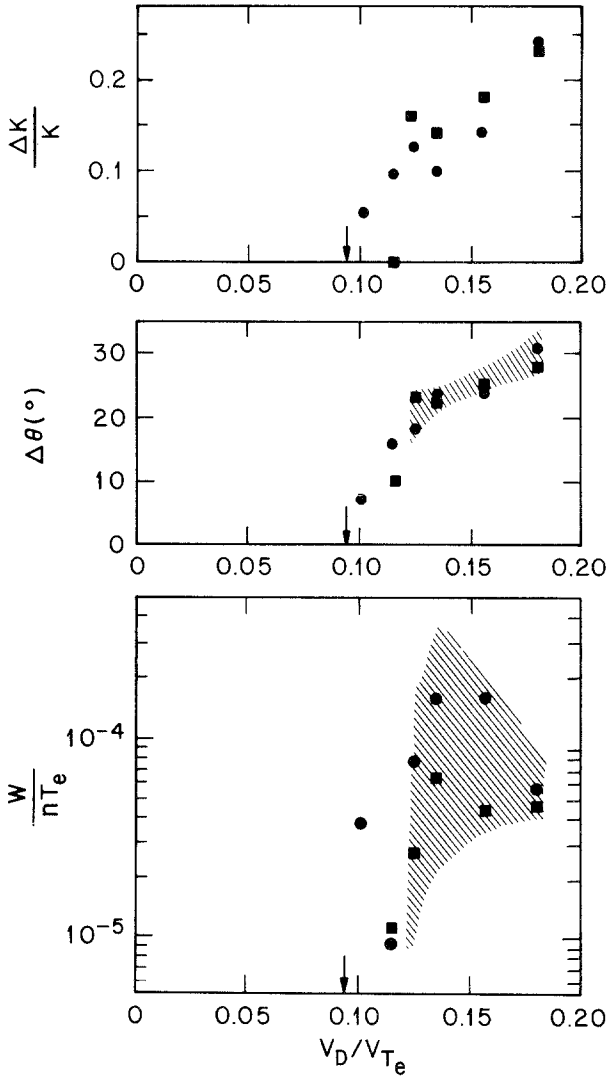

Fig. 4. The saturated level W/nT_e, the angular spread $\Delta\theta/\theta$, and wave vector width $\Delta K/K$ are shown for the saturated state of the ion acoustic instability as a function of v_D/v_{T_e}. $\Delta\theta$ and ΔK are the angular and wave vector widths, respectively, measured as the $1/e$ points of the electron fluctuation amplitude [proportional to $V(K, \theta)$ in Fig. 3]. The arrows indicate the calculated threshold values for the instability and the cross-hatched areas are calculations using an ion-resonance-broadening theory.[5] The circles and squares indicate, respectively, higher and lower values of discharge current.

(typically in the range from 0.1% to 10% of the He^+ concentration) depends on estimates of the ionization processes, changes in the H^+ impurity concentration is accurately monitored by this measurement.

The wave energy as a function of H concentration is shown in Fig. 5. These data were taken at fixed v_D/v_{T_e}. Light scattering measurements (solid circles) extend over a range of H concentrations estimated to be in the range from 1% to 6%. Above these concentrations there is no measurable level of excitation of ion acoustic waves. At the lowest level of H concentration (in Fig. 5, the open circle is an average of many runs in this region), the saturation level becomes independent of H concentration. Over the range from 1 to 6 units of hydrogen emission shown in Fig. 5, the light scattering data indicate that the angular spread of the waves is constant with $\Delta\theta \simeq 16 \pm 2°$.

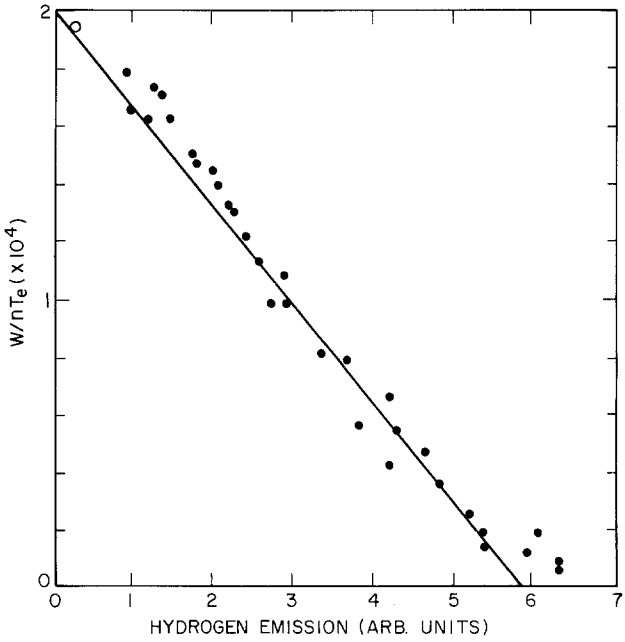

Fig. 5. The level of the saturated state of the ion acoustic instability is shown as a function of the H impurity emission in a He positive column. The units for H impurity emission for the neutral atomic line at a wavelength of 6563 Å correspond approximately to the percentage of H in the plasma. The solid circles were taken using light scattering techniques described in the text. The open circle is an average of many runs at very low concentrations of H using a dual probe where the relative level varied with H concentration in the same manner as the light scattering data. The solid line is a theoretical fit to the data described in the text.

5. DISCUSSION AND CONCLUSIONS

The strong dependence of the saturation level on a controlled concentration of H impurity ions leads one to hope that either the ion-saturation mechanisms or ion-damping processes could be better understood using the data shown in Fig. 5. An initial attempt to interpret the earlier data shown in Figs. 3 and 4 using ion-resonance-broadening theory[11] is described in Ref. 5. A reasonable fit to the angular distribution and the fluctuation level of the saturated state was obtained for a range of H concentrations over the range from 1% to 6%. The predictions for W/nT_e and $\Delta\theta/\theta$ are shown as the cross-hatched regions in Fig. 4. At present, it appears that terms were omitted from this theory which substantially reduce the effects of ion-resonance broadening to a level where it can no longer completely account for saturation of the ion acoustic growth rate.

The simple linear ion Landau damping model described in Section 2 has been suggested[2] to explain the dependence of W/nT_e on c_H. In Fig. 5, the solid line is a fit to the data using Eq. (10) and assuming that the H concentration is proportional to the hydrogen emission. It is also assumed that the nonlinear saturation mechanism is independent of both c_H and θ and that $\cos\theta \sim 1$ over the angular spread of the saturated state. This model appears to explain the major features of the data in Fig. 5: i.e., the apparent threshold near $c_H \sim 6\%$, the linear dependence of W/nT on c_H, and the saturation level at very low concentrations. The relatively large values of light-ion Landau damping significantly decreases the net growth rate. This decrease may explain some of the discrepancy between the growth rates previously measured and calculated by Yamada and Raether,[1] who found measured growth rates three times smaller than the calculated values. Most other previous experiments have been done in Pyrex tubes with no special monitoring or minimizing of H impurities.

This model, however, is too simple to explain in detail the saturated state which is observed. For example, the constant measured value of the angular spread as a function of v_D/v_e is not explained. One possible explanation of this effect is that, since the growth lengths are of the order of the discharge tube diameter, waves propagating at large angles to the tube axis do not reach saturated amplitudes. This effect might also contribute to the discrepancy between the angular spreads measured here and the very small angular spreads measured by Ilic[2] using a smaller-diameter discharge tube. It is not possible in this model to determine whether the nonlinear processes are purely electron mechanisms; however, the good agreement assuming only linear ion Landau damping and nonlinear processes independent of the light ions does point in the direction of an electron nonlinearity.

Electron trapping by the wave potential has been suggested[12] as a major contributor to the nonlinear saturation. The electron bounce frequency in a wave potential ϕ is

$$\omega_B = \left(\frac{e\phi}{m}\right)^{1/2} K \tag{11}$$

For the measured wave amplitude, $W/nT_e \sim 2 \times 10^{-4}$, this frequency is $\omega_B/2\pi \sim 150$ MHZ, which is much larger than the electron collision frequency. However, the effects of electron trapping are reduced by the angular spread of the saturated state. An electron traveling perpendicular to $\mathbf{v}_D$ will remain in a coherent wave potential for a time τ_c which can be estimated to be

$$\tau_c \sim \frac{\lambda}{v_e \Delta\theta} \tag{12}$$

At very low H concentration $\omega_B \tau_c \gtrsim 1$ and electron trapping is expected to be a major contributor to the nonlinear saturation. In earlier work at higher H concentrations,[5] the wave saturation levels were lower and the angular spreads were larger so that $\omega_B \tau_c \lesssim 1$ and electron trapping is expected to be less important.

Renormalized turbulence theories[7] have predicted saturation levels, angular spreads, and wave vector spectra in close agreement with the results presented here. It is predicted[7] that renormalization effects of the large-amplitude waves on the particle distributions become important when W/nT_e is of the order of m_e/M_i (which is 10^{-4} for the He positive column plasma). Thus, for the observed levels $W/nT_e \sim 2 \times 10^{-4}$, renormalization phenomena should be important. However, one important effect for our experiments not included in this theoretical work is ion-neutral collisions. These collisions tend to thermalize any hot ion tails created by the wave potentials. Finally, numerical simulations have not been applied to the case of positive column plasma, at least to date.

In conclusion, light scattering techniques allow a nonperturbing measurement of the saturated state level, spectrum and angular distribution of ion acoustic waves in a He-positive-column plasma. Ion acoustic waves are driven unstable by inverse Landau damping on the drifting electron distribution. Major linear damping mechanisms are found to be ion-neutral collisions and ion Landau damping on light H ion impurities in concentrations of a few percent. A major component in the nonlinear saturation is probably electron trapping in the wave potential. Ion-resonance broadening may also contribute to saturation; however, the evidence for this is not as compelling as was previously reported.[5] A complete description of the saturated state may have to include the finite geometry of the plasma

because its diameter is of the order of growth lengths for the unstable waves. Theoretically, the damping of ions in the renormalized theory remains to be studied.

ACKNOWLEDGMENTS

It is a pleasure to acknowledge useful discussions with D. B. Ilic and W. Horton, and the technical assistance of Max Rhinewine in the work to minimize the H impurity content in the plasma. We are grateful to D. Dubois and the organizing staff for inviting us to review this subject at the recent conference at Los Alamos National Laboratory on "Transport and Propagation in Nonlinear Systems."

REFERENCES

1. M. Yamada and M. Raether, *Phys. Fluids* **18**:361 (1975).
2. D. B. Ilić, *Phys. Fluids* **20**:1717 (1977).
3. R. L. Stenzel, *Phys. Fluids* **21**:93, 99 (1978).
4. W. Gekelman and R. L. Stenzel, *Phys. Fluids* **21**:609 (1978).
5. R. E. Slusher, C. M. Surko, D. R. Moler, and M. Porkolab, *Phys. Rev. Lett.* **36**:674 (1976).
6. R. E. Slusher and C. M. Surko, *Phys. Fluids* **23**:472 (1980).
7. W. Horton, Jr. and D. Choi, *Phys. Rep.* **49**:273 (1979).
8. D. Biskamp and R. Chadura, *Plasma Physics and Controlled Nuclear Fusion Research*, Vol. 2 (IAEA, Vienna, 1971), p. 265; *Phys. Rev. Lett.* **27**:1553 (1971).
9. E. L. Lindman, *J. Phys. (Paris)* **38**:9 (1977) (Collogue 66).
10. I. Alexeff, W. D. Jones, and D. Montgomery, *Phys. Rev. Lett.* **19**:422 (1967).
11. A. Sleeper, J. Weinstock, and B. Bezzerides, *Phys. Fluids* **16**:1508 (1973).
12. K. Nishikawa and C. S. Wu, *Phys. Rev. Lett.* **23**:1020 (1969).